Large Wood Transport, Deposition and Remobilization during Floods in the Czarny Dunajec River: Outcomes from Numerical Modelling

Virginia Ruiz-Villanueva, Bartłomiej Wyżga, Joanna Zawiejska, Paweł Mikuś, Hanna Hajdukiewicz, Maciej Hajdukiewicz and Markus Stoffel

Abstract The knowledge of large wood (LW) dynamics regarding factors controlling wood transport, preferential depositional sites and the timing and duration of wood flux, is crucial for the maintenance of a good ecological status of rivers and for the management of wood-related potential hazards. Besides field surveys, tracking experiments or physical modelling, numerical models represent an alternative and complementary approach to explore LW dynamics, to test hypotheses

V. Ruiz-Villanueva (✉) · M. Stoffel
Dendrolab.ch, Institute of Geological Sciences, University of Bern,
Baltzerstrasse 1+3, 3012 Bern, Switzerland
e-mail: virginia.ruiz@dendrolab.ch

M. Stoffel
e-mail: markus.stoffel@dendrolab.ch

B. Wyżga · P. Mikuś · H. Hajdukiewicz
Institute of Nature Conservation, Polish Academy of Sciences,
al. Mickiewicza 33, 31-120 Kraków, Poland
e-mail: wyzga@iop.krakow.pl

P. Mikuś
e-mail: mikus@iop.krakow.pl

H. Hajdukiewicz
e-mail: hanahaj@gmail.com

B. Wyżga · P. Mikuś
Faculty of Earth Sciences, University of Silesia, ul. Będzińska 60, 41-200 Sosnowiec, Poland

J. Zawiejska
Institute of Geography, Pedagogical University of Cracow,
ul. Podchorążych 2, 30-084 Kraków, Poland
e-mail: zawiejska.joanna@gmail.com

M. Hajdukiewicz
Department of Environmental Engineering, Geomatics and Energetics, Kielce University of Technology, Al. Tysiąclecia Państwa Polskiego 7, 25-314 Kielce, Poland
e-mail: mhajdukiewicz@gmail.com

Z.W. Kundzewicz et al. (eds.), *Flood Risk in the Upper Vistula Basin*,
GeoPlanet: Earth and Planetary Sciences, DOI 10.1007/978-3-319-41923-7_6

and to run scenarios. We used a 2D numerical model which simulates the transport of large wood together with flow dynamics. The model is able to predict and simulate wood transport and deposition, and reproduces interactions between wood, channel bed, floodplain surface and infrastructures. We applied this model combined with direct field observations to explore main factors controlling large wood dynamics in the Czarny Dunajec River in Poland. We simulated different types of logs under different flood magnitude scenarios (steady and unsteady flow conditions) to analyse wood transport, deposition and remobilization in two contrasting river morphologies. We summarized in this chapter the main outcomes from this work. Results illustrate that a wide range of quantitative information about LW transport and deposition can be obtained from the use of numerical modelling together with the proper assessment of inlet and boundary conditions and validation based on field data.

Keywords In-stream wood · Woody debris · Large wood dynamics · Iber-wood 2D model · Poland

1 Introduction

In forested mountain streams, the interaction between riparian vegetation and geomorphic processes is amplified by high stream power, high sediment transport rates and abundant wood delivery to the channels (Badoux et al. 2015; Rickenmann et al. 2015). Besides other parameters influencing wood distribution along the channels (e.g., recruitment processes, forest stand and age or forest and river management), geomorphology is a major control on the transport and distribution of large wood in rivers (Wohl and Cadol 2011). In addition, wood dynamics is also controlled by flow patterns (Gurnell 2012). Flood frequency and magnitude are significant factors influencing the distribution of large wood in rivers (Moulin et al. 2011). However, the knowledge about transport, deposition and remobilization processes of large wood within fluvial corridors is still limited because of a lack of accurate field data (MacVicar et al. 2009; MacVicar and Piégay 2012). In spite of that, researchers have tried to understand the hydraulic conditions at which wood movement occurs, proposing empirical and conceptual models relating river morphology and hydraulic parameters to the frequency and size of wood (Benda and Sias 2001), examining the influence of wood on flow resistance (Wilcox and Wohl 2006; Allen and Smith 2012), or running physical modelling experiments (Braudrick and Grant 2000, 2001; Bocchiola et al. 2002; Haga et al. 2002; Schmocker and Hager 2011; Welber et al. 2013; Bertoldi et al. 2014). These studies have demonstrated that wood transport may be more complicated than sediment transport (Wohl and Cadol 2011; MacVicar and Piégay 2012), and therefore more knowledge is still needed.

A variety of techniques have been employed to measure wood retention: detailed mapping of the locations of wood pieces (Elosegi et al. 1999), remote sensing

(Lassettre et al. 2008; Bertoldi et al. 2013), wood tagging and tracking (MacVicar et al. 2009) and physical experiments (Bertoldi et al. 2014). This chapter shows another approach to analysing wood dynamics by combining numerical modelling and field measurements. A wide range of quantitative information about wood transport and deposition can be obtained from the use of numerical modelling together with the proper assessment of boundary conditions and validation based on field data (Ruiz-Villanueva et al. 2016a, b, c). In this work we combine the numerical simulation of wood transport and deposition with field observations to analyse wood dynamics along the mountainous Czarny Dunajec River in southern Poland. This river has been studied in detail in regard to wood storage, which gives an excellent opportunity to verify and compare field observations and modelling results. As numerical modelling was run here in a multi-run mode, the results can be analysed in a probabilistic manner. This chapter summarizes main outcomes from the combination of numerical modelling with information obtained from field surveys and tracking of wood in the river. The goals were to determine main factors controlling wood transport, depositional patterns of large wood that may result from the occurrence of floods of different magnitude, and the impacts of flood sequencing as well as to analyse relationships with flow regime and discharge.

2 Study Site: The Czarny Dunajec River

The Czarny Dunajec (Fig. 1) is a gravel-bed river mostly draining the Inner Western Carpathians; it originates at about 1500 m a.s.l. in the high-mountain Tatra massif, with the highest peak in the catchment at 2176 m a.s.l. Hydrological regime of the river is determined by the high-mountain part of the catchment and is typified by low winter flows and floods occurring between May and August as a result of prolonged frontal rains, sometimes superimposed on snow-melt runoff. Mean annual discharge of the river is 4.4 $m^3\ s^{-1}$ at Koniówka, in the middle course of the river (catchment area of 134 km^2) and 8.8 $m^3\ s^{-1}$ at Nowy Targ (432 km^2), close to the confluence of the Czarny Dunajec and the Biały Dunajec rivers.

As a result of spatially variable human impacts over the past few decades (Zawiejska and Wyżga 2010), the river varies highly in width and morphology. This allows distinction of two different reaches: a single-thread, partially channelized reach 1 and an unmanaged, multi-thread reach 2 (Fig. 1). The total length of the study reaches is 5.5 km. In reach 1 the river has relatively small, uniform width, and a few drop structures reduce slope locally. One or both channel banks are reinforced with gabions or rip rap. In reach 2 the width of the active river zone amounts to 116 m on average, but it varies considerably from 60 m at the upstream end of the reach, where islands are small and scarce, to about 180 m near its downstream end where islands consequently become more important (Mikuś et al. 2013). The substantial differences in river width between the reaches are reflected in markedly different unit stream power of flood flows and in higher average flow

Fig. 1 Location of the Czarny Dunajec River (*in red*) and the location and appearance of the study reaches. Flow direction in the photos is towards the camera for reach 1 and out of the camera for reach 2

depth in the narrower reach 1. Moreover, the differences in channel management and river morphology underlie differences in the intensity of LW recruitment and the availability of LW retention sites between the reaches (Wyżga and Zawiejska 2005, 2010).

The river banks in both reaches as well as the forested islands in reach 2 are overgrown with forest stands composed of alder and willow species, with predominating young, shrubby forms of *Alnus incana*, *Salix eleagnos, S. purpurea* and *S. fragilis*, less frequent stands of older *A. incana* trees and occasional *S. alba* trees (Mikuś et al. 2013). With riparian tree height reaching 18 m, the study reaches represent large channels with respect to in-stream wood (Wyżga et al. 2015; cf. Gurnell et al. 2002; Wohl 2013).

3 Methods

The wood transport module of 2D hydrodynamic model *Iber* has been tested in real rivers in previous works (Ruiz-Villanueva et al. 2014a, b), and thus only a brief description is provided here.

Wood incipient motion is considered performing a balance of forces (i.e. the gravitational force acting in a downstream direction; the friction force in the direction opposite to flow; and the drag force, also acting in the flow direction) acting on each single piece of wood (assuming logs as cylinders). Some of the parameters involved in the governing equations are: wood density, angle of the log relative to flow, log length, log diameter, friction coefficient between the wood and the river bed and the drag coefficient of the wood in water. The method couples the flow variables calculated with the hydrodynamic module to update the position and velocity of the wood logs at every time step. The movement of logs includes two possible transport mechanisms (i.e. floating or sliding) based on wood density; and both translation and rotation, the latter reflecting the fact that one end of a piece of wood is moving faster than the other end (based on flow velocity field). Interactions between logs and the channel configuration and among logs themselves are also taken into account in the model. The influence of wood on hydrodynamics can be, in general terms, expressed as a reduction of the average velocity and local elevation of the water surface profile (Gippel 1995); it is solved in the model similarly to the effect of roughness—by including an additional shear stress term in the 2D Saint Venant equations. Therefore, flow conditions exert an influence on the logs but also the presence of logs affects the flow. In order to incorporate wood transport into the model, initial wood and boundary conditions need to be established.

The model works with a non-structured mesh of elements which may have 3 or 4 sides. To obtain this non-structured mesh, the detailed geometry of the entire reach was produced with available digital elevation models (DEM) and a topographical survey aimed at improving the DEM in those sections where its accuracy was insufficient (i.e. critical sections such as bridges, dikes or bends). As a result, we obtained detailed (1 m spatial accuracy) geometry of the studied reaches.

Data from the Koniówka stream gauging station was used to characterise the inlet flow. This station is located 6.2 km upstream of the study reaches. Data was used first for the calculation of flood discharges of a given probability/recurrence interval (for running different inlet discharge scenarios) before the available rating curve was used for roughness (Manning’s n) calibration. Roughness coefficient was obtained from the delineation, both in the channel and the flooding areas, of homogeneous land units in terms of their roughness (roughness homogeneous units; RHU) and by using in situ measurements of bed material size in selected channel transects (Wyżga et al. 2012, Zawiejska et al. 2015). Each RHU delimited in the field was digitized in ArcGIS and assigned a possible range of roughness values, following the criteria of Chow (1959) and applying different empirical equations (Meyer-Peter and Müller 1948; Bray 1979; Strickler 1923) in transects. Different discharge ranges were run to calibrate the obtained values of Manning roughness coefficient for high and low flows and to estimate assumed errors.

Wood characteristics used in the simulations were based on the riparian vegetation in the Czarny Dunajec (Table 1). In the model runs, we varied log length (L_w), log diameter (D_w) and wood density (ρ_w). Wood density was assigned between 0.4 and 0.7 g cm^{-3}, except for type 1. In order to simulate the lack of buoyancy for type 1 of wood, we assumed very high wood density (0.85–0.95 g cm^{-3}). In addition, a sensitivity analysis of this factor was also carried out (Ruiz-Villanueva et al. 2016c).

Significant floods occurred recently in the Czarny Dunajec River, namely in 2001, 2010, and 2014. Field observations regarding wood transport and deposition were made after these floods, with published results for the flood of 2001 (Wyżga and Zawiejska 2005, 2010). The data obtained during these post-flood surveys allow validation, interpretation and discussion of model results. In addition, during the most recent flood in May 2014 (peak discharge of 130 m^3 s^{-1} with a 20-year recurrence interval at the Koniówka gauging station), 30 logs tagged with radio transmitters (length: 3 m; diameter: ca. 20 cm) were placed into the river just before the flood peak. Tracking of these logs allowed further analysis of wood transport during this relatively high-magnitude flood. The flood magnitude was high enough for the flow to overtop the reach 1, and activate all low-flow channels and inundate gravel bars and islands in reach 2.

The analysis of the factors controlling wood transport was based on the transport ratio. The transport ratio, Tr, is defined as the ratio between the outlet and inlet number of logs (Tr = pieces transported downstream the studied reach/total inlet logs) and it is inverse to the wood retention capacity: Rc = deposited logs/inlet logs; ($Tr = 1 - Rc$).

4 Results and Discussion

4.1 Large Wood Transport

One of the first aspects we explored was the dependence of wood transport on log volume. We combined diameters and lengths (always within a reliable range based on vegetation and wood in the Czarny Dunajec) resulting in different piece volumes, and simulated them under different flow conditions (different steady discharges). We observed that the number of pieces in transport (defined here by the transport ratio) strongly decreased with increasing piece volume (Fig. 2a, b). However, the scatter of points in Fig. 2 shows that this relationship is not linear but can be better explained by a power function. A significant relationship (p-value < 0.01) was identified between the quantities of transported wood and the volume of the pieces in motion. The scatter in the diagrams is because different discharges resulted in different transport ratios for the same piece volume. According to our results, the scatter is higher in reach 1, especially for larger piece volumes (Fig. 2a). In addition, we

Table 1 Wood characteristics used in the simulations and based on the riparian vegetation in the Czarny Dunajec

Type of simulated logs	Length (m)	Diameter (m)	Wood density (gr cm^{-3})
1. Large alders (*Alnus incana*) and mature willows (*Salix eleagnos*)	10–18	0.3–0.8	0.85–0.95
2. Very large willows (*Salix fragilis* and *S. alba*)	10–15	0.15–0.3	0.4–0.7
3. Young willows (*S. purpurea* and *S. eleagnos*) and alder (*A. incana*)	3–10	0.1–0.2	
4. Branches and small pieces	1–3	0.05–0.1	

observed that the two reaches also differ in the mean and maximum transport ratios. The mean transport ratio is lower in reach 2 (the wide, multi-thread channel; mean transport ratio: 0.26, SD: 0.16) than in reach 1 (the single-thread channel; mean transport ratio: 0.43, SD: 0.20). The maximum transport ratio in reach 2 is 0.57, while for reach 1 the highest value is 1, meaning that all input logs are transported downstream the reach. These values are in the range observed by other researchers. Cadol and Wohl (2010) reported mobility rates ranging between 0.8 and 0.59 in tropical headwater streams. Wohl and Goode (2008) found average mobility ranging from 0.16 to 0.23 in streams in the Rocky Mountains, while Schenk et al. (2014) reported mobility of 0.41 in a large low-gradient river. Recently Iroumé et al. (2015) reported ratios of wood mobility up to 0.28 in headwater streams in the Andes.

Moreover, the lower transport capacity of reach 2 is indicated by the fact that pieces larger than 3 m^3 in volume are not mobilized even under very high-flow conditions, whereas in reach 1 very large pieces (>6 m^3) are still in transport (Fig. 2). The results clearly show that logs of similar dimensions behave differently in both reaches as a consequence of the differences in channel geometry and hydrodynamics (flow energy and therefore transport capacity). This was confirmed during field surveys when a majority of the large wood deposited immediately downstream of the single-thread channel was observed to be highly disintegrated and abraded, indicating that the wood pieces were transported long distances (Wyżga and Zawiejska 2005).

Differences in the transport ratios show differences in the transport capacity between river reaches with different geomorphic configurations. Braided or wide multi-thread channels (reach 2) show a higher retention capacity than narrower single-thread channels (reach 1), as observed and reported by other researchers in similar fluvial environments. In the Tagliamento River in Italy, wood storage was observed to differ significantly between different geomorphic configurations (island-braided and bar-braided reaches; van der Nat et al. 2003; Bertoldi et al. 2013), whereas in the Piave River (Italy), Pecorari (2008) reported higher storage in braided as compared to wandering reaches. Also during flume experiments the crucial role of local-scale morphology in wood dispersal was observed (Welber et al. 2013).

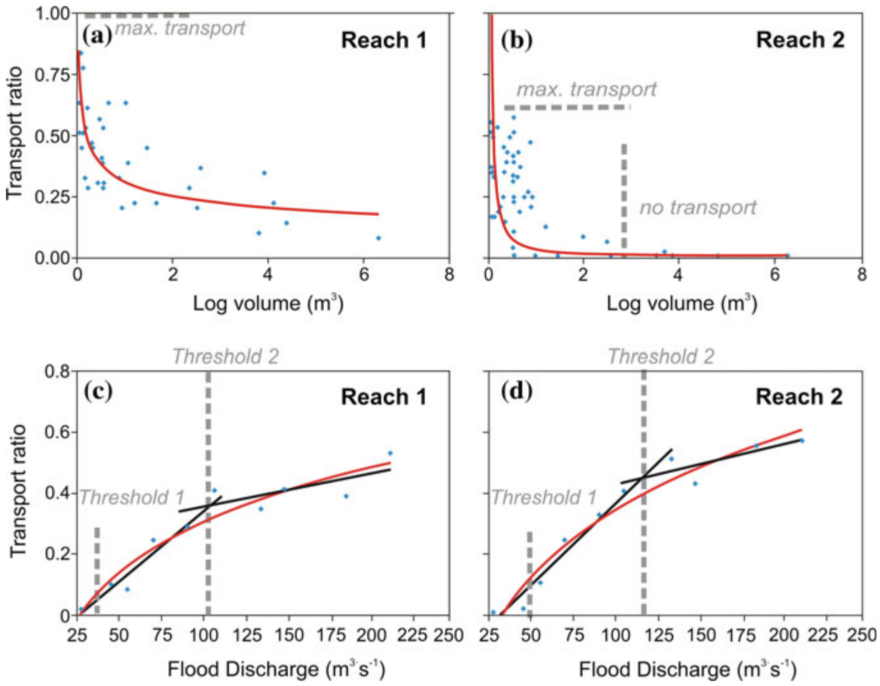

Fig. 2 Scatter plots and estimated regression relationships between large-wood transport ratio and piece volume for (**a**) the single-thread reach 1 and (**b**) the multi-thread reach 2, and between wood transport ratio and simulated flood discharges in (**c**) the single-thread reach 1 and (**d**) the multi-thread reach 2. Wood piece diameter is 0.23 m; wood piece length 12.5 m; wood density 0.56 g cm^{-3}

Besides the type of wood and river morphology, wood transport is controlled by hydrodynamics. We observed variation in wood transport ratios for the same type of logs transported under different flood magnitudes (Fig. 2c, d). The threshold discharge below which wood transport is negligible is different in each reach. In reach 1, discharges ≥ 28 m^3 s^{-1} (very frequent floods) have the capacity to transport wood, while in the multi-thread reach 2 discharges above 45 m^3 s^{-1} are needed for wood transport. In the narrow reach 1, a flow of 28 m^3 s^{-1} has enough energy and water depth to mobilize wood, whereas in the much wider reach 2 the energy and depth of the same flow are not sufficient for wood entrainment. Besides this, transport ratio increases with discharge in both reaches until it reaches an upper threshold, and then decreases and/or increases much more slowly (Fig. 2). This upper threshold is also different for each reach because is related to the bankfull discharge. For the single-thread reach 1, wood transport ratio increases rapidly with discharge until the bankfull stage is reached. At floods of higher magnitude, water begins to inundate the floodplain and a proportion of wood pieces are directed onto the channel banks where flow is shallow and slow, so that most logs will be deposited. In reach 2, once all channels are flooded, the flow over the bars and floodplains will become shallow and slow, so that wood entering these areas cannot be transported and is deposited. However, a higher discharge is required for such situation to occur in reach 2. Similar nonlinear relationships between wood transport and discharge were observed in other rivers, such as the Erlenbach and the Ain, after floods of different magnitude (MacVicar and Piégay 2012; Turowski et al. 2013).

Previous studies demonstrated that the mobility of large wood is a function of the relation between the length of pieces and channel width (Gurnell 2003). Ratios of average piece size to channel dimensions (i.e. the ratios of average piece length to channel width and of average piece diameter to flow depth), may be used to characterise the likelihood of wood mobility (Lienkaemper and Swanson 1987; Braudrick and Grant 2001). Differences in geomorphology between the studied reaches translate to differences in the hydrodynamic context, such as deeper flow, higher velocity, and higher stream power in reach 1. These differences allow the transport of thicker pieces in reach 1, whereas in reach 2 logs with a diameter similar to water depth are not moved at all (Fig. 3). Figure 3 shows that in reach 2 the slope of the linear relationship between the transport ratio and log diameter is steeper and, therefore, log diameter plays a more important role in wood transport than in reach 1 (Fig. 3b, d).

In reach 1, very short pieces (1 m long) are easily transported by the simulated flood (105 $m^3 s^{-1}$). However, for longer pieces (up to 17 m) the transport ratio decreases significantly (Fig. 3a). This relationship is not the same for reach 2 (Fig. 3c) where longer pieces (between 8 and 16 m) are more readily transported than shorter pieces (up to 8 m), whereas for very long logs (from 16 up to 22 m) the transport ratio is reduced. Longer wood pieces are generally less likely to be deposited in this reach, although a more detailed inspection of results for this scenario reveals a more complicated pattern. Shorter pieces (up to 8 m) are more easily deposited than longer pieces (between 8 and 16 m) as the flow readily introduces shorter pieces to shallow channel areas, whereas longer pieces, with greater momentum, tend to be transported along the thalweg. In turn, very long logs (from 16 m up to 22 m) are also easily deposited in reach 2 as their length facilitates their anchoring on the margins of particular braids.

Flume experiments also suggested that for braided rivers the strongest control on piece stability is wood diameter (Braudrick and Grant 2000; Welber et al. 2013). As we observed in our study and described by Ruiz-Villanueva et al. (2016c), the main factor controlling wood transport in the single-thread channel is wood piece length (Fig. 3a). On the contrary, in the multi-thread reach the main factor controlling wood transport is piece diameter (Fig. 3d).

4.2 Large Wood Deposition

Geomorphic units which are more likely to retain LW within rivers have been previously reported (Piégay et al. 1999; Gurnell et al. 2000b; Montgomery et al.

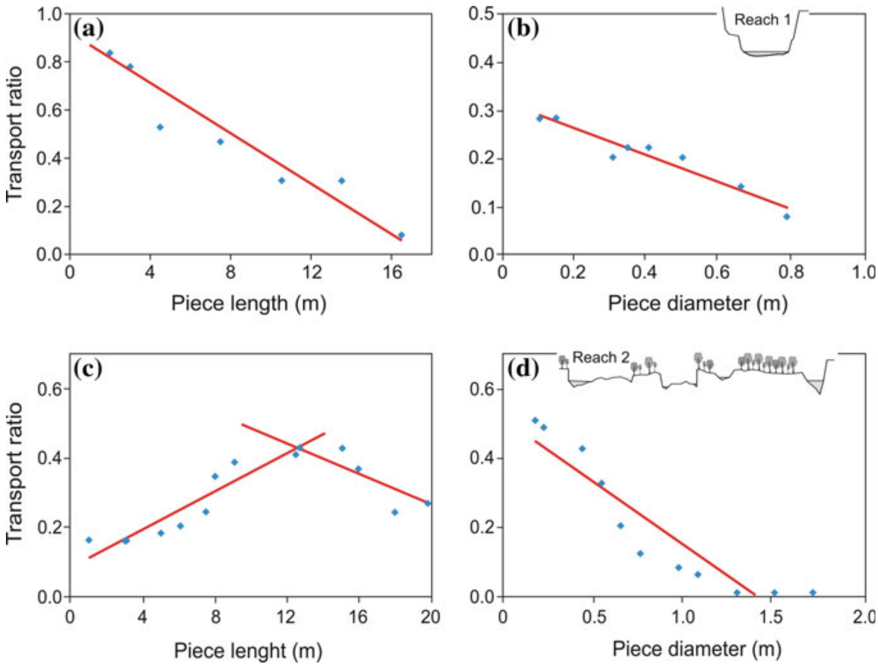

Fig. 3 **a**, **c** Relationships between wood transport ratio and the piece length for **a** the single-thread reach 1 and **c** the multi-thread reach 2. The results are shown for the simulation of the 10-year flood (105 $m^3\ s^{-1}$) and wood pieces with mean diameter of 0.2 m but different lengths (Lw) ranging from 1 to 20 m. **b**, **d** Relationships between wood transport ratio and the piece diameter for **b** the single-thread reach 1 and **d** the multi-thread reach 2. The results are shown for the simulation of the 10-year flood (105 $m^3\ s^{-1}$) and wood pieces with mean length of 12.5 m but different diameters (Dw) ranging from 0.1 to 0.8 m. Wood density is 0.56 g cm^{-3} in all cases

2003). According to our findings, LW is more likely to be deposited along the main channel, on point bars and in the forested areas adjacent to the main channel during ordinary floods (>10-year recurrence interval) in single-thread channel configurations. In multi-thread reaches, ordinary floods will tend to deposit LW on bars as well as vegetated and forested islands (Fig. 4). These preferential sites for LW deposition were identified based on the probability of deposition computed by the ensemble of the results from the multi-run model approach. Figure 4 demonstrates that for each flood scenario and for each river geomorphic configuration, different values and different spatial distributions were obtained in terms of depositional probability.

Figure 5 shows that in the case of single-thread reach 1 and for high-frequency floods, the preferential sites for LW deposition are the main channel, bars and the forested areas adjacent to the main channel. As flood magnitude increases, the probability for LW to be deposited in the main channel of reach 1 decreases. LW is likely to be transported downstream of this reach or to be deposited in the areas covered by mature forest along the floodplain. During very extreme floods, water

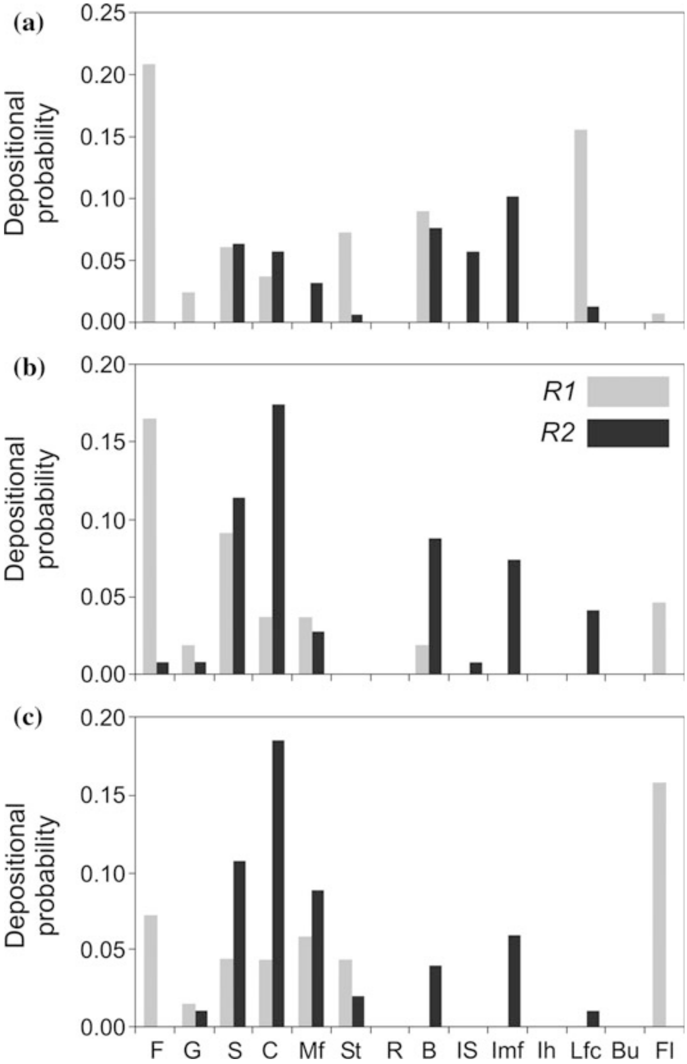

Fig. 4 **a**, **b**, **c** Depositional probability values for different RHU: Forest (F), gravelly and sandy surfaces within the floodplain (G), shrubs (S), meadows/cultivated (C), mature forest (Mf), road (R), scattered trees (St), gravel bars without vegetation (B), vegetated island (Is), forested island (Imf), island with shrubs (Ih), low-flow channel (Lfc), floodplain (Fl); and for different flood scenarios: **a** frequent floods; **b** ordinary floods; **c** very extreme floods. R1 is reach 1 and R2 is reach 2

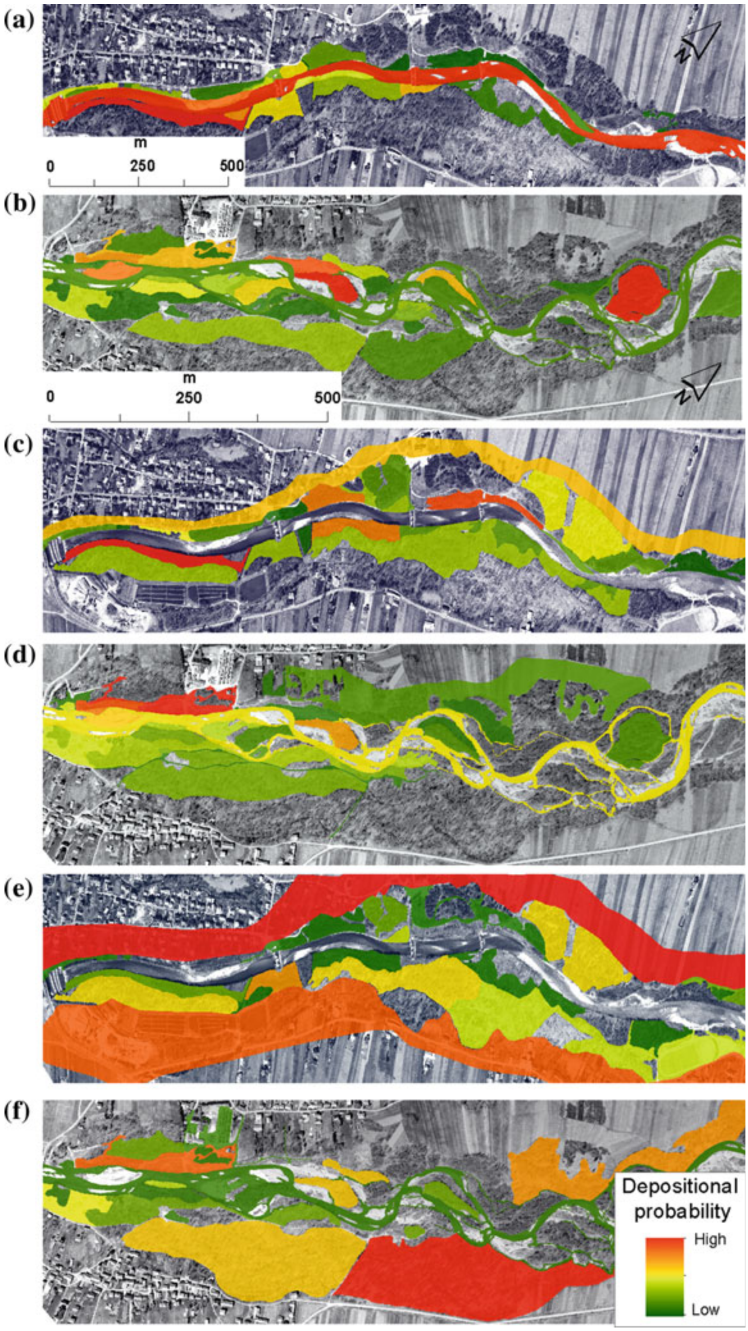

Fig. 5 Maps of wood depositional probability values for different RHU at frequent flood (1.2-year flood with a peak discharge of 28 $m^3 s^{-1}$) in Reach 1 (**a**) and Reach 2 (**b**), at ordinary flood (10-year flood; 105 $m^3 s^{-1}$) in Reach 1 (**c**) and Reach 2 (**d**), and at very extreme flood (80-year flood; 210 $m^3 s^{-1}$) in Reach 1 (**e**) and Reach 2 (**f**). Flow direction is from left to right

inundates the floodplain and a proportion of wood pieces are directed onto the channel banks where the flow is slow and shallow.

In the case of the multi-thread reach 2, during frequent floods bars, vegetated islands, and forested islands are the preferential sites for LW deposition. LW generally is not deposited on the floodplain during frequent floods. In the case of ordinary floods, LW is preferentially deposited on forested islands, in mature forest and crops on the floodplain, and along the margins of braids. During very extreme floods ($Q = 210\ m^3\ s^{-1}$), LW is retained far away from the main channel and the active river zone, in areas covered by meadows and crops as well as mature forest.

Correlation coefficients between LW depositional probability and individual controlling variables (tested by the Spearman rank correlation test) indicate that LW depositional probability is related to log dimensions (length and diameter), wood density, Manning roughness coefficient of depositional sites and flow velocity. However, only log diameter and surface roughness influence the probability of LW deposition in both reaches and under different flood conditions. Flow velocity has an influence on wood deposition only in the case of low flood flows and in reach 1 (Table 2).

The dependence of depositional probability on multiple controlling variables was verified by means of generalized multiple regression analysis (linear regression models that allow for variables with non-normal distribution of residuals). The obtained models explain between 12 and 44 % of the variation in LW depositional

Table 2 Results of the Spearman rank correlation analysis between wood depositional probability and controlling variables at the sites with LW deposits in reach 1 and reach 2 and for very frequent and very extreme flood scenarios. After Ruiz-Villanueva et al. (2016a), reproduced with permission of Wiley.

Flood magnitude	Very frequent flood		Very extreme flood	
Independent variable	Spearman correlation coefficient	*p*-value	Spearman correlation coefficient	*p*-value
Reach 1				
Wood density ($g\ cm^{-3}$)	0.156	0.043	*−0.031*	0.797
Piece diameter (m)	0.283	0.007	*−0.229*	0.057
Piece length (m)	0.147	0.057	*−0.180*	0.137
Manning roughness coefficient ($m^{1/2}\ s^{-1}$)	0.638	<0.001	*−0.219*	0.068
Flow velocity ($m\ s^{-1}$)	*	*	0.011	0.927
Reach 2				
Wood density ($g\ cm^{-3}$)	*−0.160*	0.044	*−0.358*	<0.001
Piece diameter (m)	*−0.283*	<0.001	*−0.458*	<0.001
Piece length (m)	*−0.324*	<0.001	*−0.488*	<0.001
Manning roughness coefficient ($m^{1/2}\ s^{-1}$)	0.258	0.001	*−0.468*	<0.001
Flow velocity ($m\ s^{-1}$)	*−0.336*	<0.001	0.088	0.380

Negative correlation is highlighted in italics. Water depth was not included among the independent variables because similar to flow velocity*, water depth equalled zero at most deposition locations probability, and point to the decisive role of either log length or log diameter, and surface roughness. At the same time, however, we observe that the direction of the relationship differs between low- and high-magnitude floods. For low flood flows, depositional probability is higher in the areas with higher roughness within the flooded area. In the case of very extreme floods in reach 1, the LW depositional probability is negatively related to both Manning coefficient and log diameter. The depositional probability is thus higher in the areas with low surface roughness. The negative relation between depositional probability and log diameter can be explained by the fact that with the mean length of simulated pieces at 12.5 m, even thin logs can interact easily with and be anchored on the margins of the narrow, single-thread channel. By contrast, in the case of shorter pieces, interactions with the channel margins are less likely and the ratio between log diameter and water depth is high enough to allow their downstream transport, even if the logs have large diameters.

In the case of low flood flows ($Q = 28\ m^3\ s^{-1}$) in multi-thread reach 2, the variation of depositional probability was also higher in the areas with higher roughness within the flooded area; however, a much lower proportion of the total variance can be explained by this variable.

In the scenario describing a very extreme flood ($Q = 210\ m^3\ s^{-1}$) in reach 2, the variation in depositional probability is negatively related to surface roughness. This observation again reflects the fact that at the extreme discharge LW is mostly deposited in the areas with lower values of roughness coefficient (i.e. on the floodplain). With equal roughness of depositional surfaces, logs of larger diameter are less likely to be deposited in the reach. This may reflect the fact that thicker logs tend to be transported by the flow along deeper areas with the faster current as a result of their greater momentum.

Therefore, not only roughness controls wood deposition. There has been little information in the literature on the elevation at which LW is deposited in rivers (Gurnell et al. 2000a; Bertoldi et al. 2013). Based on the results of the model runs, we indicate that the relative elevation of LW deposits differs between floods of different magnitude and we also show that LW is not always deposited in those geomorphic units where the highest roughness values occur (as it occurs at low-magnitude floods). We tested the relative elevation of LW depositional sites with respect to (i) the low-flow water surface and (ii) the lower river bank. These relative elevations were analyzed for each reach and for different peak discharges (Ruiz-Villanueva et al. 2016a). For all flood magnitudes, the average elevation of LW deposits above the low-flow water surface is higher in the single-thread reach 1 (with its narrow and deep channel) than in the multi-thread reach 2 (with its wide and shallower channel). In both reaches, the relative elevation of LW deposits changes significantly with changing flood magnitude. In a similar way, elevation of LW deposits relative to the lower river bank also depends significantly on flood magnitude. However, if the relative elevation of LW deposits is considered, differences between the two reaches apparently increase with increasing flood magnitude, but become statistically significant once a certain flood magnitude is attained. Overall, these results demonstrate that LW deposition is strongly controlled by water depth (Ruiz-Villanueva et al. 2016a).

4.3 Large Wood Remobilization

In the previous sections we assumed that wood was entering the studied reaches from upstream, but previously deposited wood can be mobilized during subsequent floods (Haga et al. 2002; Wohl and Goode 2008). As observed by MacVicar and Piégay (2012), two consecutive floods with similar peak discharges and volumes mobilized different quantities of wood; as a result of antecedent flood effects, the second flood transported significantly less wood. We analysed wood remobilization using the output from a simulated flood (i.e., the resultant spatial distribution of wood) as an input for the next flood scenario without the supply of wood recruited from upstream. Results of these runs showed that the number of remobilized wood pieces is smaller in reach 1 than in reach 2 (Fig. 6) and remobilized logs travelled larger distance in reach 1 than in reach 2 (Fig.7).

One of the reasons for the greater ratio of wood remobilization from reach 2 was the magnitude of the preceding flood—consequently; in this reach the flood deposited wood pieces mostly within the active river zone. If the previous flood was greater, more pieces might be deposited on the floodplain in reach 2 and the disparity in wood remobilization ratio between the reaches might be reduced, eliminated, or maybe reversed, depending on the magnitude of the antecedent flood. We thus emphasize the importance of the magnitude of the preceding flood in predisposing the potential of deposited wood for remobilization during a subsequent flood.

4.4 Large Wood Dynamics Under Unsteady Flow Conditions

A significant feature of wood dynamics is its temporal dimension, and it is represented by simulating the entire flood hydrograph (i.e., unsteady flows). To design the hydrographs, we used the Dimensionless Unit Hydrograph method of the Soil Conservation Service (SCS 1972). This method uses the ratio between the discharge at one time step and the peak discharge ($Q \cdot Qp^{-1}$) and the ratio between time and the time to peak ($t \cdot tp^{-1}$) to build the final hydrograph. Subsequently we modified the resultant common hydrographs (i.e. the hydrographs with the most common shape in the river) to obtain flashy and flattened flood waves with the same flow volume. We defined the common flood scenario ($Q \cdot Qp^{-1} = 1$ and $t \cdot tp^{-1} = 1$) where the flood peak is reached 5 h after the beginning of the flood wave, and the total flood duration equals 25 h. In the flattened flood wave scenario ($Q \cdot Qp^{-1} = 0.5$ and $t \cdot tp^{-1} = 2$), floods have a total duration of 35 h and the peak is

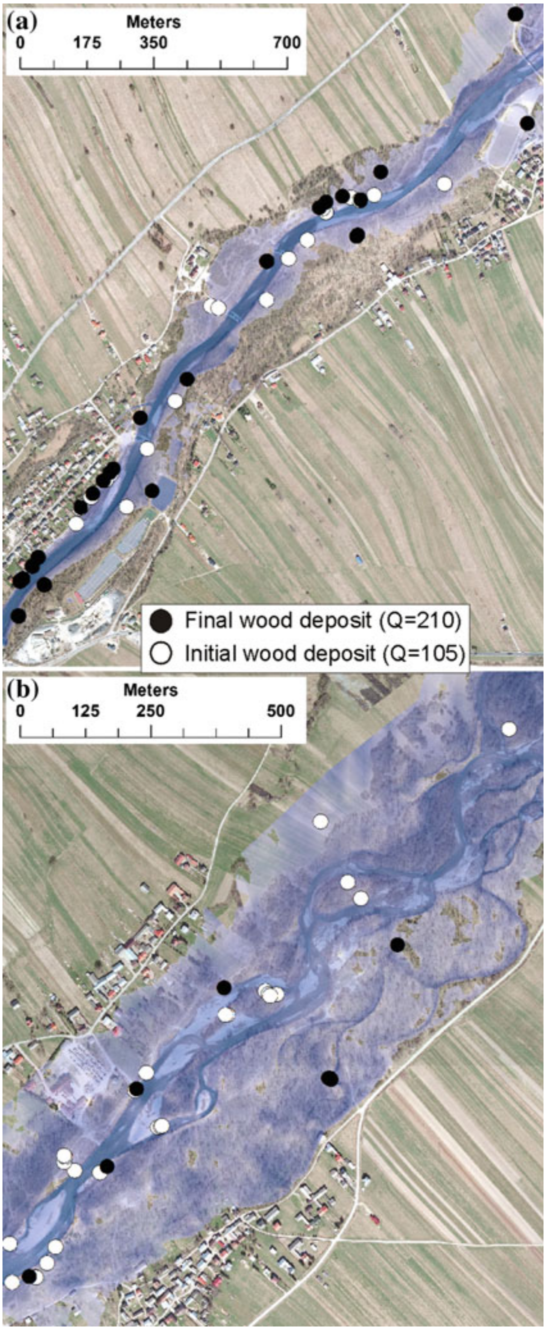

Fig. 6 Logs stored at the initial flood (Q = 105 m^3 s^{-1}; *white dots*) and final flood (Q = 210 m^3 s^{-1}; *black dots*) in reach 1 (**a**) and reach 2 (**b**). Flooded area of final flood is mapped in *blue*

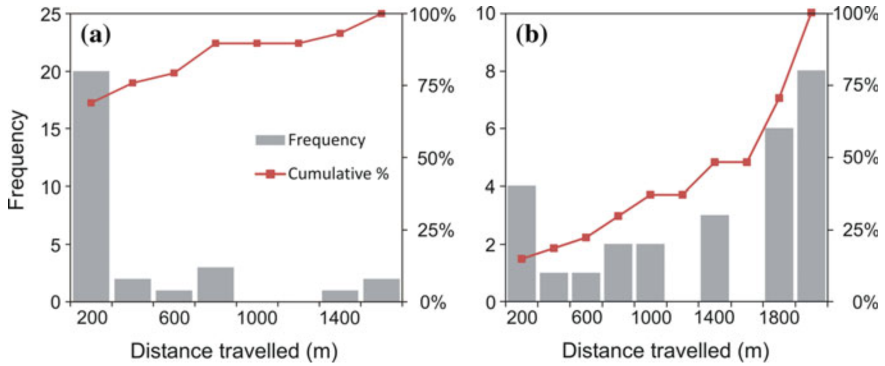

Fig. 7 Distribution of travelled distance (i.e. distances between the locations of remobilization and deposition of the remobilized logs, including those which exited the modelling domain) for Reach 1 (**a**) and Reach 2 (**b**)

reached after 10 h, whereas in the flashy flood scenario ($Q \cdot Qp^{-1} = 1.5$ and $t \cdot tp^{-1} = 0.5$) floods last for 17 h and the peak is passing after 3 h. In all scenarios, the shape of the hydrographs reflects the shape of flood waves occurring in the river, with a rising limb being steeper than the falling limb. In this set of modelling tests, we also analysed wood remobilization, using the result of the simulated discharge of 28 $m^3 \cdot s^{-1}$ (1.2-year flood) as an initial condition. Therefore, we assumed that wood recruitment is not occurring upstream from the study reaches or laterally (due to bank erosion), but that only the initially deposited wood is being remobilized.

Results of the simulated hydrographs showed that large wood is transported downstream during the rise of the hydrograph, and we observed a time lag between the beginning of the flood and wood motion (Fig. 8). The peak of the wood flux is systematically reached before the flood peak in all scenarios and in both reaches (Fig. 8 shows just three cases). This observation is in agreement with Schenk et al. (2014) who state that most wood is mobilized at the very beginning of the flood in the Roanoke River. This result was confirmed by Ravazzolo et al. (2015) who, in addition, observed that most of their tagged logs in the Tagliamento River were deposited right at the flood peak.

Our findings also confirmed that wood transport decreases near or slightly after hydrograph peaks. This suggests that the mobilization of in-stream wood is likely negligible during the falling limb of the hydrograph as wood has already been subject to the same or larger discharges during the flood rise. All these observations might be of great interest to manage potential wood-related hazards during floods.

Common and flashy hydrographs with higher peak discharges mobilized more logs than the equivalent flattened floods. A 5-year flood with the common hydrograph shape and the flattened equivalent of a 25-year flood have similar peak discharges (78 $m^3 \cdot s^{-1}$ and 73 $m^3 \cdot s^{-1}$, respectively) but a slightly higher percentage of mobilized wood is associated with the latter, despite its slightly lower peak discharge. On the other hand, a 25-year flood with a common hydrograph is

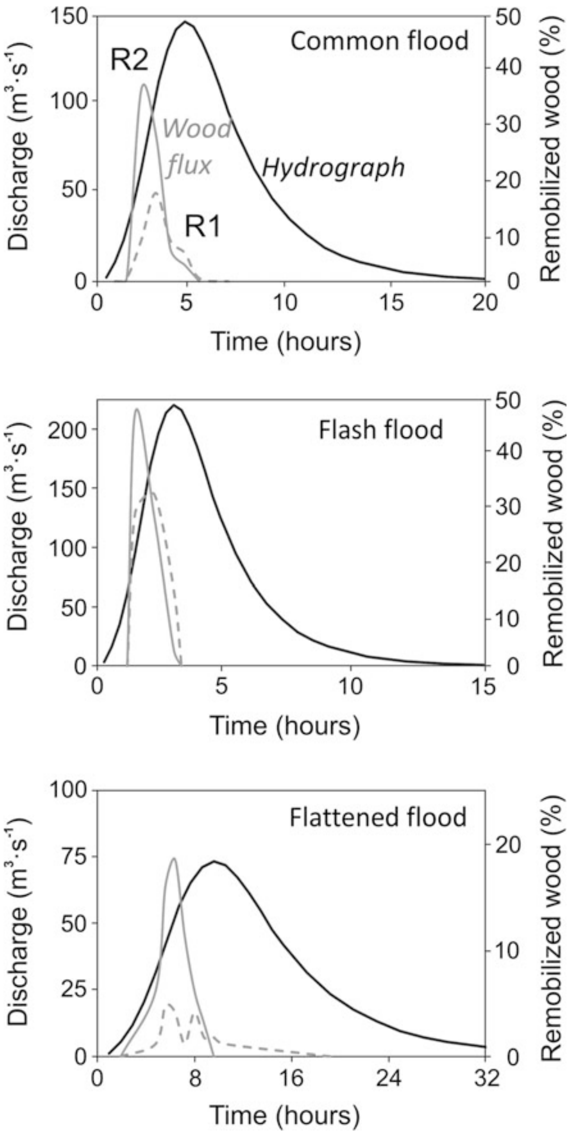

Fig. 8 Flood hydrographs (*black solid lines*) and temporal variation in the mobilization of initial wood pieces (in %) in reach 1 (R1; *dashed grey lines*) and reach 2 (R2; *solid grey lines*)

able to transport a smaller number of pieces downstream from the reaches than the flashy equivalent of the 5-year flood, even though the former has a higher peak discharge. Therefore, the hydrograph shape and the duration of the flood also significantly influence the mobilization of in-stream wood and its duration.

While the number of mobilized logs was positively related to flow peak, the length of wood mobilization period is negatively related to peak discharge, but positively to the duration of the flood, particularly to the time to peak. As we observed when we simulated large wood transport under steady-flow conditions, the relationships between wood transport and the time to peak and between wood transport and the peak discharge of the flood are not linear (Ruiz-Villanueva et al. 2016b). The highest wood flux occurs during flashy floods which generally have higher peak discharges, and the lowest flux is associated with the equivalent flattened flood scenarios (Fig. 9). The common hydrograph scenarios represent an intermediate situation (Fig. 9).

The transport of wood commences during the rising limb and ceases before the peak of the flood wave in the flash flood scenario, whereas it extends into an early phase of flood recession in both reaches in the flattened flood scenario (Fig. 9). Here, the largest pieces are moved during the flood peak, whereas in the case of the flash flood with a higher discharge, the largest pieces are already transported before the peak (Fig. 9). When both reaches are compared, we observe that floods in reach 2 move pieces of smaller sizes than in reach 1. This is because of differences in water depth and flow velocity between the reaches.

Wood transport in rivers is a nonlinear process, and the relation between the proportion of mobilized wood and discharge during (simulated) floods is complex (Ruiz-Villanueva et al. 2016b). In-stream wood starts to move as soon as a certain discharge is reached, and in the case of previously deposited wood, this threshold is clearly related to the magnitude of the antecedent flood. In both cases, the number

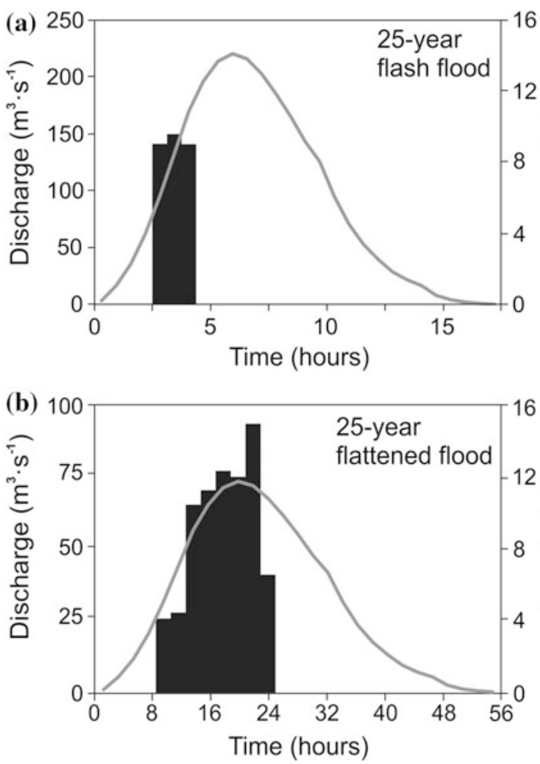

Fig. 9 Flood hydrographs (*grey line*) and the length of mobilized wood pieces (*black histogram*) in reach 1 during the flashy (**a**) and flattened (**b**) equivalents of the 25-year flood

of mobilized pieces increases with increasing discharge until the maximum amount of transported wood is reached. After this point, and even if discharge is still increasing, the number of wood pieces in motion will decrease and eventually the motion will cease completely. We attribute this phenomenon to the hysteresis (Ruiz-Villanueva et al. 2016b) in mobilization of wood pieces with discharge as previously proposed by Marcus et al. (2011) and MacVicar and Piégay (2012).

5 Concluding Remarks

The results of this study help to understand the complex relationships between floods and wood motion, despite the fact that several relevant processes that occur at the field scale—such as sediment transport and bank erosion—could not be considered in the modelling approach. Moreover, still only very limited information is available on the actual mechanics of wood recruitment and transport within streams, such that we still do not know how the timing of individual tree fall, mass recruitment, jam formation or jam breakup will correspond to flow hydrographs (Wohl et al. 2011). Despite these limitations and possible shortcomings, we remain convinced that the results from this study can be generalized and therefore extrapolated to other rivers with similar characteristics.

After decades of modelling sediment transport the knowledge is far from complete, so there is still a long way to travel and several challenges to be met to fully understand wood transport, even more for combining both processes. Recent advances in computer technology have increased our capabilities for developing more detailed, computationally intensive models. Similarly, advances in GIS technologies and field-measurement equipment and techniques have provided extensive and highly accurate data, and allowed for modelling, analysis, and monitoring of wood transport over various spatial and temporal scales. An integrated framework, combining several of those techniques would help improve the theoretical and numerical models of wood transport and allow for performing more extensive testing and validation of these models. Thus, it would allow for comprehensive understanding of the transport processes, their influence on hydrodynamics and geomorphology and the spatial and temporal environmental variability.

The knowledge of wood dynamics and the outcomes regarding timing and duration of wood load transport and the influence of flood hydrograph presented in this paper are crucial for developing adaptive management of the potential hazards of LW to human communities and infrastructure, both in the Czarny Dunajec valley (cf. Kundzewicz et al. 2014) and elsewhere.

Acknowledgments This work was supported by the project FLORIST (Flood risk on the northern foothills of the Tatra Mountains; PSPB no. 153/2010). Authors acknowledge the revision made by Dr. Walter Bertoldi which improved the early version of this chapter.

References

Allen JB, Smith DL (2012) Characterizing the impact of geometric simplification on large woody debris using CFD. J Hydraul Eng 1:1–14

Badoux A, Böckli M, Rickenmann D, Rickli C, Ruiz-Villanueva V, Zurbrügg S (2015) Large wood transported during the exceptional flood event of 24 July 2014 in the Emme catchment (Switzerland). In: Picco L, Lenzi MA, Bertoldi W et al (eds) Proceedings of the third international conference 'Wood in world rivers 3', Padova, Italy, pp 109–111

Benda LE, Sias JC (2001) A quantitative framework for evaluating the mass balance of in-stream organic debris. Forest Ecol Manag 172:1–16

Bertoldi W, Gurnell AM, Welber M (2013) Wood recruitment and retention: the fate of eroded trees on a braided river explored using a combination of field and remotely-sensed data sources. Geomorphology 180:146–155

Bertoldi W, Welber M, Mao L, Zanella S, Comiti F (2014) A flume experiment on wood storage and remobilization in braided river systems. Earth Surf Proc Landforms 39:804–813

Bocchiola D, Catalano F, Menduni G, Passoni G (2002) An analytical-numerical approach to the hydraulics of floating debris in river channels. J Hydrol 269:65–78

Braudrick CA, Grant GE (2000) When do logs move in rivers? Water Resour Res 36:571–583

Braudrick CA, Grant GE (2001) Transport and deposition of large woody debris in streams: a flume experiment. Geomorphology 41:263–283

Bray DI (1979) Estimating average velocity in gravel-bed rivers. J Hydr Div 105:110–1122

Cadol D, Wohl E (2010) Wood retention and transport in tropical, headwater streams, La Selva Biological Station, Costa Rica. Geomorphology 123:62–73

Chow VT (1959) Open-channel hydraulics. McGraw-Hill, New York

Elosegi A, Díez JR, Pozo J (1999) Abundance, characteristics and movement of woody debris in four Basque streams. Arch Hydrobiol 147:455–471

Gippel CJ (1995) Environmental hydraulics of large woody debris in streams and rivers. J Environ Eng 121:388–395

Gurnell AM (2003) Wood storage and mobility. In: Gregory SV, Boyer KL, Gurnell AM (eds) The ecology and management of wood in world rivers. Am Fish Soc Symp 37:75–91

Gurnell AM (2012) Wood and river landscapes. Nat Geosci 5:93–94

Gurnell AM, Petts GE, Hannah DM, Smith BPG, Edwards PJ, Kollmann J, Ward JV, Tockner K (2000a) Wood storage within the active zone of a large European gravel-bed river. Geomorphology 34:55–72

Gurnell AM, Petts GE, Harris N, Ward JV, Tockner K, Edwards PJ, Kollmann J (2000b) Large wood retention in river channels: the case of the flume Tagliamento, Italy. Earth Surf Proc Landforms 25:255–275

Gurnell AM, Piégay H, Swanson FJ, Gregory SV (2002) Large wood and fluvial processes. Freshwater Biol 47:601–619

Haga H, Kumagai T, Otsuki K, Ogawa S (2002) Transport and retention of coarse woody debris in mountain streams: an in situ field experiment and a field survey of coarse woody debris distribution. Water Resour Res 38:11–26

Iroumé A, Mao L, Andreoli A, Ulloa H, Ardiles M (2015) Large wood mobility processes in low-order Chilean river channels. Geomorphology 228:681–693

Kundzewicz ZW, Stoffel M, Kaczka RJ, Wyżga B, Niedźwiedź T, Pińskwar I, Ruiz-Villanueva V, Łupikasza E, Czajka B, Ballesteros-Canovas J, Małarzewski Ł, Choryński A, Janecka K, Mikuś P (2014) Floods at the northern foothills of the Tatra Mountains—A Polish-Swiss Research Project. Acta Geophys 62:620–641

Lassettre NS, Piégay H, Dufour S, Rollet A (2008) Decadal changes in distribution and frequency of wood in a free meandering river, the Ain River, France. Earth Surf Proc Landforms 33:1098–1112

Lienkaemper GW, Swanson FJ (1987) Dynamics of large woody debris in streams in old-growth Douglas-fir forests. Can J Forest Res 17:150–156

MacVicar BJ, Piégay H (2012) Implementation and validation of video monitoring for wood budgeting in a wandering piedmont river, the Ain River (France). Earth Surf Proc Landforms 37:1272–1289

MacVicar BJ, Piégay H, Henderson A, Comiti F, Oberlin C, Pecorari E (2009) Quantifying the temporal dynamics of wood in large rivers: field trials of wood surveying, dating, tracking, and monitoring techniques. Earth Surf Proc Landforms 34:2031–2046

Marcus WA, Rasmussen J, Fonstad MA (2011) Response of the fluvial wood system to fire and floods in Northern Yellowstone. Ann Assoc Am Geogr 101:21–44

Meyer-Peter E, Müller R (1948) Formulas for bed-load transport. Proceedings of the 2nd meeting of the international association for hydraulic structures research, pp 39–64

Mikuś P, Wyżga B, Kaczka RJ, Walusiak E, Zawiejska J (2013) Islands in a European mountain river: linkages with large wood deposition, flood flows and plant diversity. Geomorphology 202:115–127

Montgomery DR, Collins BD, Buffington JM, Timothy BA (2003) Geomorphic effects of wood in rivers. In: Gregory SV, Boyer KL, Gurnell AM (eds) The ecology and management of wood in world rivers. American Fisheries Society Symposium 37:21–47

Moulin B, Schenk ER, Hupp CR (2011) Distribution and characterization of in-channel large wood in relation to geomorphic patterns on a low-gradient river. Earth Surf Proc Landforms 36:1137–1151

Pecorari E (2008) Il materiale legnoso in corsi d'acqua a canali intrecciati: volumi, mobilità, degradazione ed influenza morfologica. PhD thesis, University of Padova, Italy

Piégay H, Thévenet A, Citterio A (1999) Input, storage and distribution of large woody debris along a mountain river continuum, the Drôme River, France. Catena 35:19–39

Ravazzolo D, Mao L, Picco L, Lenzi MA (2015) Tracking log displacement during floods in the Tagliamento River using RFID and GPS tracker devices. Geomorphology 228:226–233

Rickenmann D, Waldner P, Usbeck T, Köchil D, Sutter F, Rickli C, Badoux A (2015) Large wood transport during the 2005 flood events in Switzerland. In: Picco L, Lenzi MA, Bertoldi W et al (eds) Proceedings of the third international conference 'Wood in world rivers 3', Padova, Italy, pp 124–126

Ruiz-Villanueva V, Bladé E, Díez-Herrero A, Bodoque JM, Sánchez-Juny M (2014a) Two-dimensional modelling of large wood transport during flash floods. Earth Surf Proc Landforms 39:438–449

Ruiz-Villanueva V, Bladé E, Sánchez-Juny M, Marti-Cardona B, Díez-Herrero A, Bodoque JM (2014b) Two-dimensional numerical modelling of wood transport. J Hydroinform 16:1077–1096

Ruiz-Villanueva V, Wyżga B, Hajdukiewicz H, Stoffel M (2016a) Exploring large wood retention and deposition in contrasting river morphologies linking numerical modelling and field observations. Earth Surf Proc Landforms 41:446–459

Ruiz-Villanueva V, Wyżga B, Mikuś P, Hajdukiewicz H, Stoffel M (2016b) The role of flood hydrograph in the remobilization of large wood in a wide mountain river. J Hydrol. doi:10.1016/j.jhydrol.2016.02.060

Ruiz-Villanueva V, Wyżga B, Zawiejska J, Hajdukiewicz M, Stoffel M (2016c) Factors controlling large wood transport in a mountain river. Geomorphology 272C. doi:10.1016/j.geomorph.2015.04.004

Schenk ER, Moulin B, Hupp CR, Richter JM (2014) Large wood budget and transport dynamics on a large river using radio telemetry. Earth Surf Proc Landforms 39:487–498

Schmocker L, Hager WH (2011) Probability of drift blockage at bridge decks. J Hydraul Eng 137:480–492

SCS (1972) Soil conservation service. National engineering handbook, section 4. U.S. Department of Agriculture, Washington, DC

Strickler A (1923) Beiträge zur Frage der Geschwindigkeitsformel und der Rauhigkeitszahlen für Ströme, Kanäle und geschlossene Leitungen. Mitteilungen des Amtes für Wasserwirtschaft 16, Bern

Turowski JM, Böckli M, Rickenmann D, Beer A (2013) Field measurements of the energy delivered to the channel bed by moving bed load and links to bedrock erosion. J Geophys Res Earth Surf 118:2438–2450

Van der Nat D, Tockner K, Edwards PJ, Ward JV, Gurnell AM (2003) Habitat change in braided flood plains (Tagliamento, NE-Italy). Freshwater Biol 48:1799–1812

Welber M, Bertoldi W, Tubino M (2013) Wood dispersal in braided streams: results from physical modeling. Water Resour Res 49:7388–7400

Wilcox AC, Wohl E (2006) Flow resistance dynamics in step-pool stream channels: 1. Large woody debris and controls on total resistance. Water Resour Res 42:1–16

Wohl E, Goode JR (2008) Wood dynamics in headwater streams of the Colorado Rocky Mountains. Water Resour Res 44:W09429

Wohl E (2013) Floodplains and wood. Earth-Sci Rev 123:194–212

Wohl E, Cadol D (2011) Neighborhood matters: patterns and controls on wood distribution in old-growth forest streams of the Colorado Front Range, USA. Geomorphology 125:132–146

Wohl E, Polvi LE, Cadol D (2011) Wood distribution along streams draining old-growth floodplain forests in Congaree National Park, South Carolina, USA. Geomorphology 126:108–120

Wyżga B, Zawiejska J (2005) Wood storage in a wide mountain river: case study of the Czarny Dunajec, Polish Carpathians. Earth Surf Proc Landforms 30:1475–1494

Wyżga B, Zawiejska J (2010) Large wood storage in channelized and unmanaged sections of the Czarny Dunajec River, Polish Carpathians: implications for the restoration of mountain rivers. Folia Geogr Ser Geogr-Phys 41:5–34

Wyżga B, Oględki P, Radecki-Pawlik A, Skalski T, Zawiejska J (2012) Hydromorphological complexity as a driver of the diversity of benthic invertebrate communities in the Czarny Dunajec River, Polish Carpathians. Hydrobiologia 696:29–46

Wyżga B, Zawiejska J, Mikuś P, Kaczka RJ (2015) Contrasting patterns of wood storage in mountain watercourses narrower and wider than the height of riparian trees. Geomorphology 228:275–285

Zawiejska J, Wyżga B (2010) Twentieth-century channel change on the Dunajec River, southern Poland: patterns, causes and controls. Geomorphology 117:234–246

Zawiejska J, Wyżga B, Radecki-Pawlik A (2015) Variation in surface bed material along a mountain river modified by gravel extraction and channelization, the Czarny Dunajec, Polish Carpathians. Geomorphology 231:353–366